PERGAMON

Vision Research 38 (1998) 3843–3848

Vision Research

Geometric representation of the mechanisms underlying human curvature detection

David Whitaker *, Paul V. McGraw

Department of Optometry, University of Bradford, Richmond Road, Bradford, West Yorkshire BD7 1DP, UK

Received 26 November 1997; received in revised form 16 March 1998

Abstract

Combined manipulation of blur, line length and contrast reveal two distinct processes involved in curvature detection. When line length is small relative to blur, thresholds are almost directly proportional to blur and independent of line length. When line length is large relative to blur thresholds are directly proportional to line length and independent of blur. The aspect ratio (line length/blur) of curved contours represents a scale-invariant metric which forms the decisive factor in determining curvature performance. © 1998 Elsevier Science Ltd. All rights reserved.

Keywords: Hyperacuity; Curvature

1. Introduction

The design of the human visual system confers an acute ability to make judgements regarding shape, depth and location. In studies of one such judgement, it has been found that curved lines can be discriminated from straight lines to within approximately one fifth of the physical spacing between two neighbouring cones and one tenth of the smallest receptive field centre of ganglion cells [1–4]. This level of performance has led to curvature discrimination being placed amongst the set of spatial discriminations given the group label of hyperacuities [5].

Curved lines play an important role in object recognition. Indeed, the perceptual potency of contour curvature was demonstrated by Attneave [6]. By identifying only the points of maximum curvature and joining them with straight lines he showed that objects (in this case a sleeping cat) could still be recognised. This example highlights the important role played by curvature in both shape representation and recognition. Furthermore, contour curvature discrimination also plays an influential role in social behaviour where it provides salient information for both face recognition and the interpretation of facial expressions [7].

Riggs [8,9] made the assertion that the detection of curvature was a primary goal of visual analysis and that this information was processed on a global basis via cortical neurones selective to curvature [10–12]. Subsequently, endstopping, or selectivity of cortical neurones for stimulus length, has been suggested as a substrate for estimating curvature [13–15]. Models of curvature processing have also examined how this type of judgement may be achieved by way of local orientation selective mechanisms. This approach has been embraced in the model of Wilson and Richards [16] who theorise a scheme where local mechanism responses can accurately predict thresholds for high degrees of curvature (steep curves). However, at low curvatures a non local process is required which utilises the responses of filters displaced a known distance along the tangent of the curved contour. This model suggests a transition from a local pattern discrimination strategy to a global strategy as the curvature of the contour is decreased, which consequently extends the range of curvatures over which accurate curvature discrimination is possible.

With the notable exception of Hess and Watt [4], studies examining the possible mechanisms which mediate curvature detection have usually adopted a one-dimensional approach. For example, the effect of manipulating stimulus line length might be investigated whilst other stimulus attributes remain constant. If we

* Corresponding author. Fax: +44 1274 385570; e-mail: d.j.whitaker@bradford.ac.uk.

PII: S0042-6989(98)00104-7

are to fully understand the mechanisms underlying curvature discrimination we need to examine the response of the visual system to curves which vary not only in line length but also in other parameters such as blur and contrast. Perhaps a fuller understanding of the nature of curvature processing lies in a knowledge of the quantitative relationships between these factors since, in natural visual scenes, curved contours typically vary in multiple dimensions.

2. Methods

2.1. Stimuli

The stimuli consisted of horizontally-oriented line stimuli. These lines were windowed in both horizontal and vertical dimensions with a Gaussian profile. The mathematical description of the curved line stimuli is given by Eq. (1)

$$L_{\text{mean}} - \left[L_{\text{mean}} \times \text{contrast} \times \exp\left(-\left(\frac{x^2}{2\sigma_{\text{H}}^2} + \left(\frac{(y - (r - \sqrt{r^2 - x^2}))^2}{2\sigma_{\text{V}}^2} \right) \right) \right) \right] \quad (1)$$

Where L_{mean} is the mean luminance of the background, x and y are the horizontal and vertical distances from the centre of the curve, and σ_{H} and σ_{V} are the horizontal and vertical scale parameters which define stimulus length and stimulus blur, respectively. The parameter r represents the radius of curvature of the stimulus.

We examined a range of x- and y-blur levels by varying the scale parameter of the relevant Gaussian window, such that stimuli varied in appearance from long, thin lines to short fat ones (Fig. 1a). The maximum contrast of the lines was either 12.5 or 100%.

Stimuli were presented within a circular on-screen mask which had a central luminance of 71.6 cd m^{-2} and a surround luminance of 1.58 cd m^{-2}. This mask allowed the presentation of at least six horizontal standard deviations for all stimuli apart from the longest line length (256 arc min) which was truncated to 4.4 standard deviations. A control experiment using a line length of 128 arc min revealed that truncation of the stimulus in this manner had no significant influence on performance. The stimuli were generated using the macro capabilities of NIH Image 1.52 public domain software (updated versions available from the Internet by anonymous ftp from zippy.nimh.nih.gov and sunet.se.pub.mac.graphics or on a floppy from the National Technical Information service, Springfield, VA, part number PB95-500195GEI), and presented on a 17″ Apple multiple scan display with a frame rate of 72 Hz. The non-linear luminance response of the display was corrected using standard photometric procedures. The host computer was a Power Macintosh 6100/66.

2.2. Procedures

Observers were required to indicate, via a mouse response, whether the line stimuli were curved upwards or downwards. One of seven values of curvature could be randomly presented on any trial. The maximum sagitta of the line stimuli was varied to produce an appropriate ambit of responses ranging from approximately 100% upwards to 100% downwards. At least 20 trials were presented at each of the seven values of curvature, and the proportion of upwards responses was calculated. Bootstrap analysis [17] was applied to the resulting psychometric function to define the point of subjective equality (50% response level) and the threshold (difference between the 84 and 50% response levels). Curvature thresholds were defined as the sagitta to a chord length of twice the horizontal Gaussian standard deviation (Fig. 1b). All stimuli were exposed for 250 ms. The viewing distance was 69 cm and all observations were carried out under dim room illumination to avoid monitor reflections.

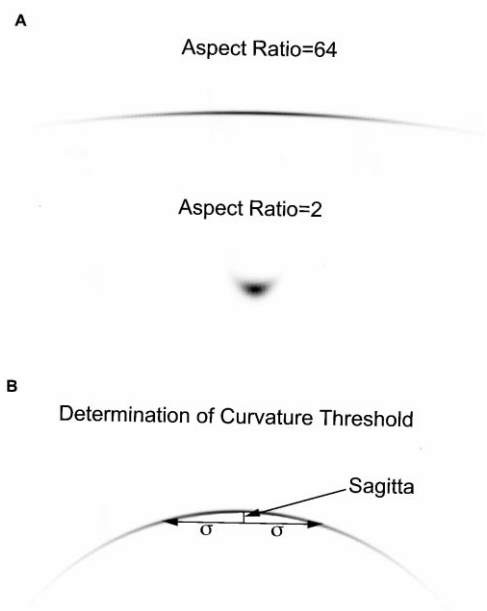

Fig. 1. Representation of high contrast curved stimuli. By varying the standard deviation of the relevant Gaussian window, the appearance of the stimuli can be varied from long, thin lines (aspect ratio = 64) to short fat ones (aspect ratio = 2). (b) Curvature thresholds are defined as the sagitta to a chord length of twice the horizontal Gaussian standard deviation.

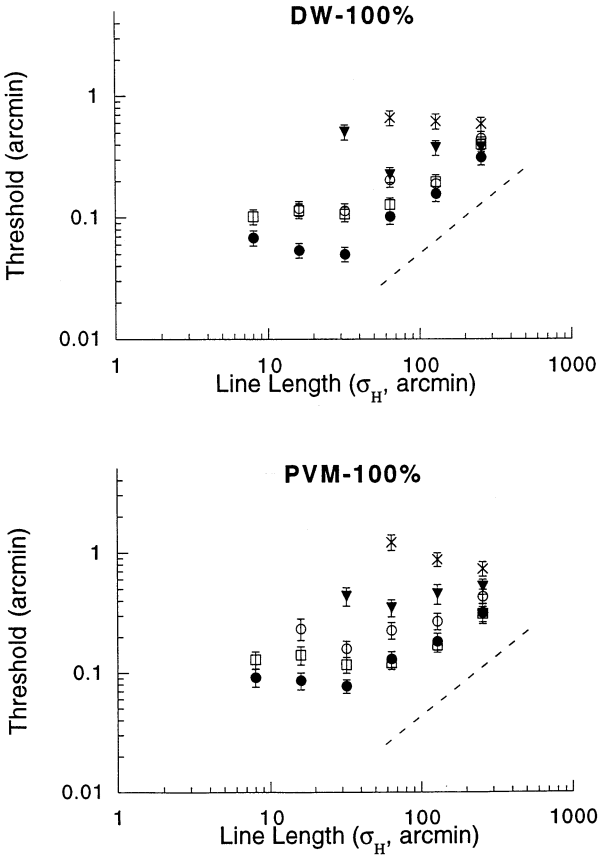

Fig. 2. Curvature thresholds for high contrast (100%) stimuli plotted against a representation of line length (horizontal Gaussian standard deviation) for a range of blur levels (vertical Gaussian standard deviation). Blur levels of 2 (filled circle), 4 (open square), 8 (open circle), 16 (filled triangle), and 32 (cross) arc min were examined. As the blur level is increased thresholds are correspondingly raised. Initially, thresholds are unaffected by line length until a kneepoint position is reached following which thresholds rise in proportion to line length. The dashed line has a gradient of one.

2.3. Observers

The two authors acted as observers in the experiment. Both observers had normal acuity (with correction for DW), were pre-presbyopic, and are highly practiced at this type of task.

3. Results

Fig. 2 shows curvature thresholds for high contrast stimuli plotted against line length (horizontal Gaussian standard deviation) for a range of blur levels (vertical Gaussian standard deviation). Line lengths varied from 8 to 256 arc min. Blur levels of 2, 4, 8, 16, and 32 arc min were examined. The results show that at a given line length thresholds increase with blur [18]. For any given blur level, the results show an initial flat region where thresholds remain constant as a function of line length, after which they increase steadily in proportion to stimulus length [4]. The dotted line on each graph has a slope of one. The knee-point at which thresholds begin to rise increases with the level of stimulus blur.

Corresponding data are shown in Fig. 3, but for the low contrast stimuli (12.5%). Comparison with Fig. 2 shows that the reduction in contrast results in increased thresholds, particularly at short line lengths.

Fig. 4 shows the data from Fig. 2 and Fig. 3 plotted together. The y-axis has now been expressed as a Weber fraction by plotting threshold as a fraction of line length. On the x-axis, line length is expressed as a fraction of the blur level of the stimulus. We have termed this metric the 'aspect ratio' of the stimulus [14]. These transformations collapse the data from different blur levels onto a single function, although the functions for the two contrast levels remain separate. The data are fitted with a function of the form:

$$W_{\mathrm{opt}^*}\sqrt{1+\left(\frac{\mathrm{AR_t}}{\mathrm{AR}}\right)^2} \tag{2}$$

where W_{opt}, and $\mathrm{AR_t}$ are constants, both of which are of interest. W_{opt} represents the optimum Weber fraction, and occurs when the aspect ratio (AR) is very

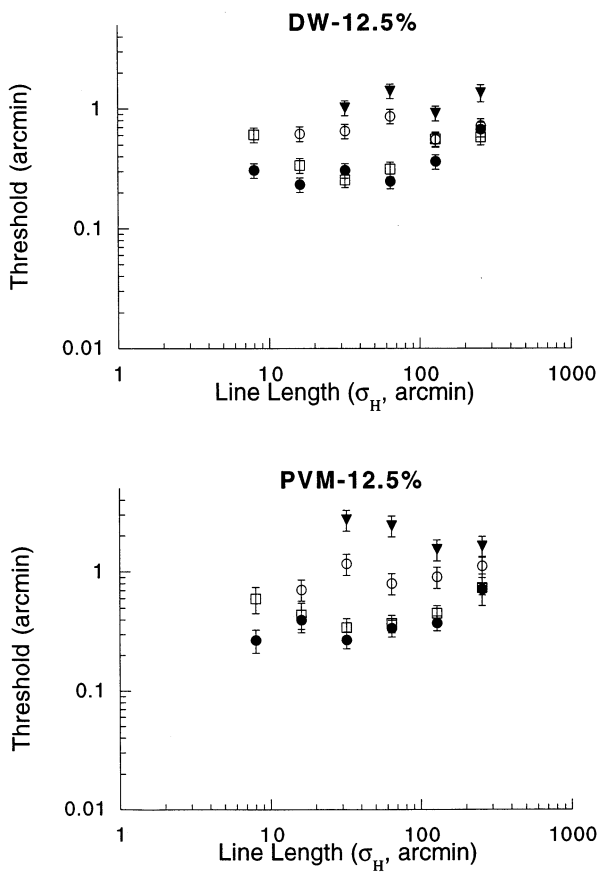

Fig. 3. A similar plot to that of Fig. 2 but at a reduced contrast level of 12.5%. Blur levels of 2 (filled circle), 4 (open square), 8 (open circle), and 16 (filled triangle) arc min were examined.

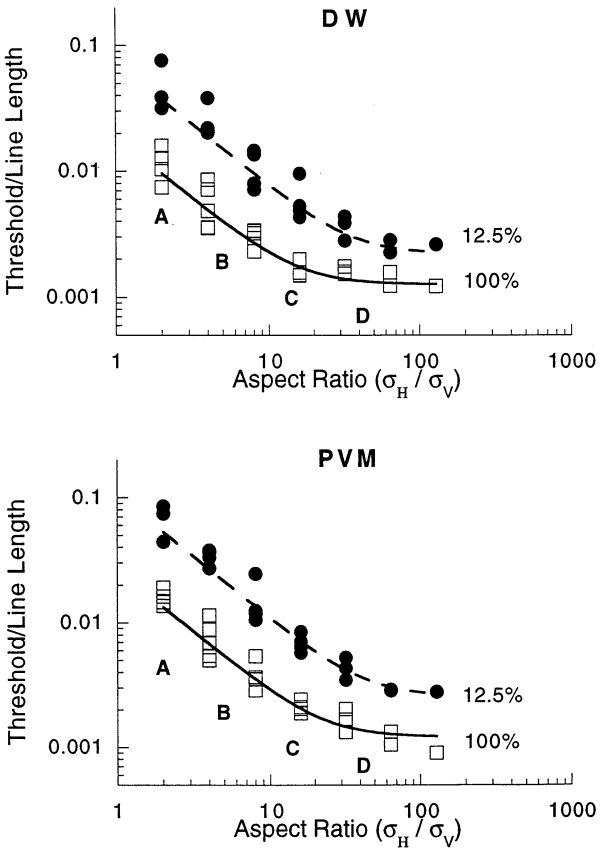

Fig. 4. Same data as in Fig. 2 and Fig. 3 but with threshold expressed as a proportion of stimulus line length (horizontal Gaussian standard deviation), and line length expressed as a proportion of stimulus blur (aspect ratio). Open squares represent the 100% contrast data of Fig. 2, filled circles the 12.5% data of Fig. 3. These transformations have the effect of collapsing data from different line lengths and blur levels together at each contrast level. A description of the curve fit is given in the text, whilst the parameters of the curve fit are shown in Table 1.

large. When the aspect ratio is very small, the Weber fraction becomes inversely proportional to the aspect ratio, or, in other words, thresholds are proportional to blur. AR_t gives an indication of the aspect ratio representing the transition from a descending Weber fraction region to a constant Weber fraction region. The values of W_{opt}, and AR_t for both observers are presented in Table 1. Standard errors for these parameter estimates are also presented. The error values for W_{opt}, are particularly pertinent due to the reduced number of data points for the higher aspect ratios, which is an unavoidable consequence of the physical limitations of the stimulus display.

4. Discussion

The data of Fig. 4 show two important regions. When line length is small relative to blur (short fat lines) thresholds are almost directly proportional to blur and independent of line length. When line length is large relative to blur (long thin lines) thresholds are directly proportional to line length and independent of blur. The results suggest that the 'aspect ratio' of the curves (the ratio of their length to their blur) is a decisive factor in determining curvature performance. Specifically, both line length and blur can limit thresholds. The 'aspect ratio' determines which of these two limiting factors dominates performance, highlighting the importance of investigating visual performance using a combination of stimulus parameters which vary in more than a single dimension.

A model which might account for the observed data is shown in Fig. 5. The rectangular boxes represent hypothetical filters which are presumed critical in providing a differential response to solve the curvature discrimination task [14,16,19]. We assume that different arrays of such filters exist, each differing in spatial scale. The four conditions depicted in Fig. 5 represent the situation at various aspect ratios A, B, C, D labelled in Fig. 4. In the region A through B to C, the stimulus blur level determines the optimum constant filter height, with the filter width increasing with stimulus line length so as to result in the same differential response. In this region the underlying filter aspect ratio is increasing to match the aspect ratio of the stimuli, thereby resulting in a constant threshold for a fixed blur level. Beyond C, filters no longer exist of sufficient aspect ratio to match the stimuli, so that filters tuned to greater blur levels (no longer matched to the stimulus blur) are invoked to provide the differential response, resulting in an increased threshold.

Our data are similar to those found in the Vernier acuity domain by Toet et al. [20]. They examined three-blob vernier acuity for Gaussian stimuli whilst varying both the blur of the individual blobs and the inter-blob separation. When the stimulus extent was small relative to the individual blob blur, thresholds were proportional to blur. However, when blur was small relative to stimulus extent, thresholds became proportional to the stimulus extent. Interestingly, the transition between the two regions occurred at a ratio of around 25, rather similar to the transitional aspect ratios found in the present results (Table 1). This may be viewed as evidence for similar underlying mechanisms in both Vernier and curvature analysis.

Fig. 4 shows that the effect of reducing stimulus contrast has a differential effect at large and small aspect ratios. At large aspect ratios, an 8-fold reduction in contrast leads to an approximate doubling of the Weber fraction (see W_{opt} values in Table 1). However, at small aspect ratios the same reduction in contrast leads to approximately a 4-fold increase in the Weber fraction. In terms of the model outlined in Fig. 5, the implication is that a reduction of contrast has a more severe effect on filters with smaller aspect ratios.

Table 1
Constant values derived from the fitting of Eq. (2) to the data

Observer	W_{opt} 100%	W_{opt} 100% S.E.	AR_t 100%	AR_t 100% S.E.	W_{opt} 12.5%	W_{opt} 12.5% S.E.	AR_t 12.5%	AR_t 12.5% S.E.
DW	0.00124	0.00016	15.662	2.760	0.00241	0.00038	31.265	6.280
PVM	0.00125	0.00014	21.630	2.600	0.00246	0.00026	41.534	6.018

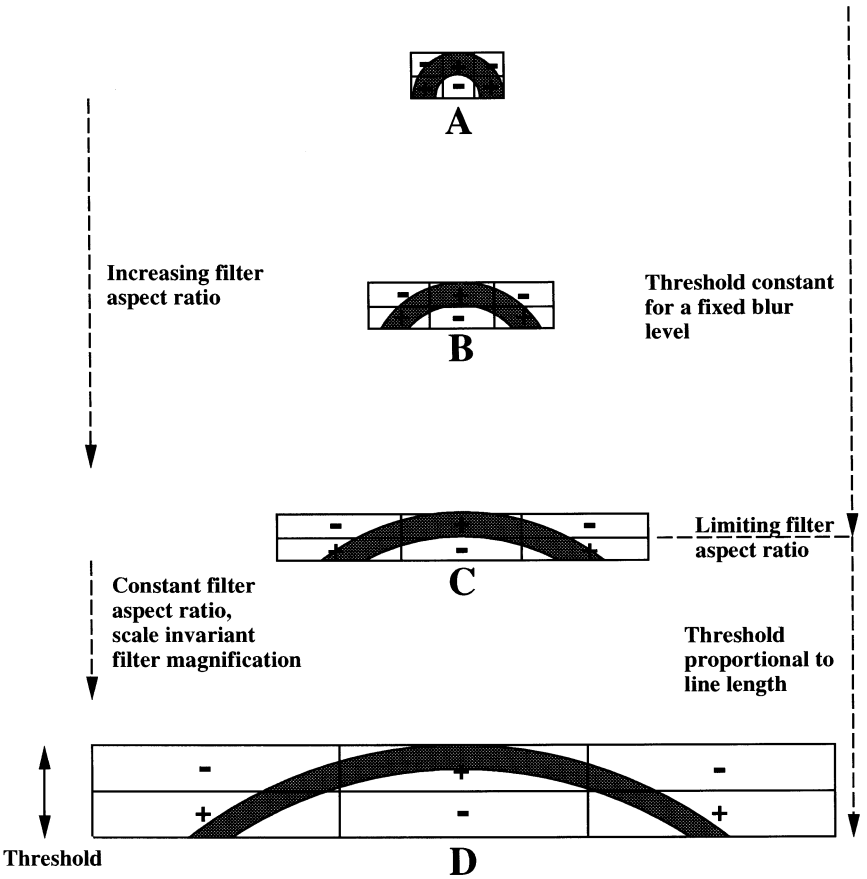

Fig. 5. A model representing curvature discrimination for different stimulus aspect ratios, labelled in Fig. 4. Filters associated with stimuli A–C all possess identical height but differ in width, thereby displaying selectivity to different stimulus aspect ratios and resulting in a constant curvature threshold defined in terms of sagitta. The filter associated with stimulus D is simply a magnified version of C resulting in an increased threshold.

The fact that the data at each respective contrast level collapse to a single function when stimulus blur and line length are accounted for (Fig. 4) is consistent with the concept of scale invariance within the visual system. In other words, any two geometrically identical curved stimuli (stimuli whose aspect ratio is the same) will be processed by geometrically identical mechanisms which differ only in terms of spatial scale (magnification). If a given stimulus has a curvature corresponding to threshold at one viewing distance, then changing viewing distance changes stimulus size in every dimension. However, the stimulus remains at threshold since it is processed by mechanisms which are simply scaled versions of the mechanisms involved at the former viewing distance. In addition to curvature discrimination [21], scale invariance also applies to many other spatial tasks [20,22,23]. The simplistic elegance of scale-invariant sensory analysis clearly represents a fundamental feature of human vision.

Acknowledgements

PVM is supported by a Vision Research Training Fellowship from the Wellcome Trust. Additional support was provided by the Visual Research Trust.

References

[1] Ogilvie J, Daicar E. The perception of curvature. Can J Psychol 1967;21:521–5.

[2] Watt RJ, Andrews DP. Contour curvature analysis: hyperacuities in the discrimination of detailed shape. Vis Res 1982;22:449–60.

[3] Watt RJ, Ward RM, Casco C. The detection of deviation from straightness in lines. Vis Res 1987;27:1659–78.

[4] Hess RF, Watt RJ. Regional distribution of the mechanisms that underlie spatial localization. Vis Res 1990;30:1021–31.

[5] Westheimer G. Spatial sense of the eye. Invest Ophthalmol Vis Sci 1979;18:893–912.

[6] Attneave F. Some informational aspects of visual perception. Psychol Rev 1954;61:183–93.

[7] Rovamo J, Mäkelä P, Näsänen R, Whitaker D. Detection of geometrical image distortions at various eccentricities. Invest Ophthalmol Vis Sci 1997;38:1029–39.

[8] Riggs RA. Curvature as a feature of pattern vision. Science 1973;181:1070–2.

[9] Riggs RA. Curvature detectors in human vision? Science 1974;184:1200–1.

[10] Blakemore C, Over R. Curvature detectors in human vision? Perception 1974;3:3–7.

[11] MacKay DM, MacKay V. Do curvature-contingent chromatic after-effects require 'detectors for curvature'? Vis Res 1974;14:1285–7.

[12] Stromeyer CF. Curvature detectors in human vision? Science 1974;184:1199–200.

[13] Dobbins A, Zucker SW, Cynader MS. Endstopping in the visual cortex as a substrate for calculating curvature. Nature 1987;329:438–41.

[14] Koenderink JJ, Richards W. Two-dimensional curvature operators. J Opt Soc Am A 1988;5:1136–41.

[15] Dobbins A, Zucker SW, Cynader MS. Endstopping and curvature. Vis Res 1989;29:1371–87.

[16] Wilson HR, Richards WA. Mechanisms of contour curvature discrimination. J Opt Soc Am A 1989;6:106–15.

[17] Foster DH, Bischof WF. Thresholds from psychometric functions: superiority of bootstrap to incremental and probit variance estimates. Psychol Bull 1991;109:152–9.

[18] Watt RJ. Scanning from coarse to fine spatial scales in the human visual system after the onset of a stimulus. J Opt Soc Am A 1987;4:2006–21.

[19] Wilson HR. Responses of spatial mechanisms can explain hyperacuity. Vis Res 1986;26:453–69.

[20] Toet A, van Eekhout MP, Simons HLJJ, Koenderink JJ. Scale invariant features of differential spatial displacement discrimination. Vis Res 1987;27:441–51.

[21] Foster DH, Simmons DR, Cook MJ. The cue for contour-curvature discrimination. Vis Res 1993;33:329–41.

[22] Whitaker D, Latham K. Disentangling the role of spatial scale, separation and eccentricity in Weber's law for position. Vis Res 1997;37:515–24.

[23] Joseph JS, Victor JD, Optican LM. Scaling effects in the perception of higher-order spatial correlations. Vis Res 1997;37:3097–107.